

(13) is used.

²As one of the possible states that must be taken into account in the dipole excitation of electrons in a magnetic field, it is also necessary to consider the state

$$\psi_{11} = \frac{2r}{(2\pi)^{3/2} r_H^2} \left(2 - \frac{r^2}{r_H^2} \right) \exp\left(-\frac{r^2}{2r_H^2}\right) e^{-i\varphi}.$$

However, the matrix element for the exciting alternating field $eE_{1r} \cos \varphi$ between the states ψ_{00} and ψ_{11} vanishes:

$$\int \psi_{00} eE_{1r} \cos \varphi \psi_{11} r dr d\varphi = 0$$

as a result of integration over r .

³We are dealing with information obtained under the conditions $\tau_{11} \gg \tau$ (see (19b)).

⁴Actually, a definition of $\Delta\omega$ lower by a factor of two than $\Delta\omega$ in (30) is used in the calculation of $\Delta\omega$, in order that the value of $\Delta\omega$ in the region $n_s < n_s^*$ coincide with the value of $\Delta\omega$ from (26) and not with the classical result (18a).

¹V. S. Édel'man, Pis'ma Zh. Eksp. Teor. Fiz. **24**, 510 (1976); **26**, 647 (1977) [JETP Lett. **24**, 468 (1976); **26**, 493 (1977)].

²V. S. Édel'man, Zh. Eksp. Teor. Fiz. **77**, No. 2 (1979).

³V. B. Shikin and Yu. P. Monarkha, Zh. Eksp. Teor. Fiz. **65**, 751 (1973) [Sov. Phys. JETP **38**, 373 (1974)].

⁴V. B. Shikin and Yu. P. Monarkha, Fiz. Nizk. Temp. **1**, 957 (1975) [Sov. J. Low Temp. Phys. **1**, 459 (1975)].

⁵V. B. Shikin, Pis'ma Zh. Eksp. Teor. Fiz. **22**, 328 (1975) [JETP Lett. **22**, 154 (1975)].

⁶A. Cheng and P. M. Platzman, Solid Stat. Comm. **25**, 813 (1978).

⁷I. M. Lifshitz, M. Ya. Azvel' and M. I. Kaganov, Elektronnaya teoriya metallov (Electron Theory of Metals) Nauka, 1971.

⁸Yu. P. Monarkha and S. S. Sokolov, Fiz. Nizk. Temp. **5**, (1979) [Sov. J. Low Temp. Phys. **5**, (1979)].

⁹D. M. Larsen, Phys. Rev. **A135**, 419 (1964).

¹⁰L. D. Landau and E. M. Lifshitz, Kvantovaya mekhanika (Quantum Mechanics) Fizmatgiz, 1963 [Pergamon, 1968].

¹¹I. S. Gradshteyn and I. M. Ryzhik, Tablitsy integralov summ, ryadov i proizvedenii (Tables of Integrals, Sums, Series, and Products) Fizmatgiz, 1962.

¹²Yu. P. Monarkha and V. B. Shikin, Zh. Eksp. Teor. Fiz. **68**, 1423 (1975) [Sov. Phys. JETP **41**, 710 (1975)].

¹³H. Fukuyama, Solid Stat. Comm. **19**, 551 (1976).

¹⁴V. B. Shikin, Zh. Eksp. Teor. Fiz. **72**, 1619 (1977) [Sov. Phys. JETP **45**, 850 (1977)].

¹⁵F. D. Mackie and Chia-Wei Woo, Phys. Rev. **B18**, 529 (1978); Legesse Senbetu and Chia-Wei Woo, Phys. Rev. **B18**, 3251 (1978).

Translated by R. T. Beyer

Thermal conductivity of pure lead crystals at low temperatures

L. P. Mezahov-Deglin

Institute of Solid State Physics, USSR Academy of Sciences

(Submitted 29 March 1979)

Zh. Eksp. Teor. Fiz. **77**, 733-751 (August 1979)

Results are presented of measurements of the thermal conductivity of perfect and of plastically deformed crystals of pure lead (certified 99.9999% Pb) in the normal and superconducting states in the temperature interval 0.6-7.5 K. Judging from the thermal conductivity in perfect crystals of 2-4 mm diameter in a zero magnetic field, the maximum phonon mean free paths are limited by scattering from the surface, and the maximum electron mean free paths are limited by scattering from impurity atoms. In a strongly deformed sample at temperatures $T \sim 1$ K the quasiparticle free paths are limited by scattering from dislocations, and the principal role in the phonon thermal conductivity is played by the flutter effect, i.e., scattering of phonons by vibrating dislocations. At temperatures $T > 2$ K the phonon and electron mean free paths are limited by the mutual scattering of the quasiparticles. A comparison of the experimental data with the predictions of the theory of thermal conductivity of pure superconductors shows that the behavior of the phonon component of the thermal conductivity agrees in practice with the theory, while the temperature dependences of the thermal conductivity of the electronic component differ substantially from the theoretical ones.

PACS numbers: 74.30.Ek, 74.70.Gj, 72.15.Eb, 72.15.Qm

1. INTRODUCTION

This work is a continuation of a cycle of studies, initiated by us earlier,¹⁻³ of kinetic phenomena in perfect bulky crystals at low temperatures. Such investigations are essential for a better understanding of the role of various relaxation mechanisms of excitation and of energy-transport mechanisms in perfect crystalline structures at low temperature; they are also of interest from the point of view of utilitarian material study, and can serve as a basis for the production of crystals with specified physical properties, for the development of

physical methods for the analysis of highly purified materials, etc. The objects of the preceding measurements were solid helium and bismuth, a nearly perfect dielectric and semimetal, respectively, with low carrier density ($\sim 10^{-5}$ per atom), whose thermal conductivity at helium temperatures is determined by the relaxation processes in the phonon system. It was natural to choose as the next object a superconductor, since the thermal conductivity of a superconductor in the normal state, just as that of a normal metal, is determined mainly by the electronic component κ_n^0 , while in the superconducting state at $T \ll T_c$ it is determined

by the phonon (lattice component κ_p^s , since the number of electronic excitations decreases exponentially with decreasing temperature. Thus, from the results of measurements of the thermal conductivity of the superconductor it is possible to assess the properties of both the electron and the phonon system separately.

Particular interest attaches to superconductors with strong electron-phonon coupling, such as lead, mercury, or niobium, which have a relatively high critical temperature T_c and a low Debye temperature Θ ($T_c = 7.199$ K and $\Theta(0) = 100$ K in lead, and $T_c/\Theta = 0.08$, whereas e.g., in aluminum $T_c/\Theta = 0.003$). The phonon component of the thermal conductivity κ_p^s of these superconductors becomes equal to the electron component κ_e^s already at $T \leq 0.7T_c$. Since the maximum phonon thermal conductivity in a dielectric is observed at $T_{\max}/\Theta \leq 0.03$, it is clear that the maximum of phonon thermal conductivity in lead should lie below T_c at $T_{\max}/T_c \leq 0.3$, inasmuch as allowance for phonon-electron scattering can only lower the point T_{\max} .

It is thus clear beforehand that near T_c the electron component predominates in the thermal conductivity of lead, the effective transport mean free paths of the electrons are limited by electron-phonon scattering, and when the temperature is lowered the phonon component becomes predominant in the superconducting state. From the results of the measurements one can assess both the effectiveness of the mutual scattering of quasiparticles of various sorts by one another, and the scattering of the phonons and carriers by impurity atoms and lattice defects of one and the same sample, i.e., superconductors with tight binding offer unusual possibilities for the study and comparison of thermal-excitation relaxation mechanisms simultaneously in the phonon and electron systems of the investigated metal.

The thermal conductivity of lead samples at low temperature was investigated many times previously. A detailed resume and summary plots of the results of various workers are given in Ref. 4. It was shown that at temperatures $T < 5$ K in a zero magnetic field the thermal conductivity of lead is determined mainly by the phonon component κ_p^s . It was regarded as natural that below T_{\max} , at temperatures $T \leq 2$ K, the principal relaxation mechanism is the scattering of the phonons by the sample surface, while at $T > T_{\max}$ it is the scattering by electronic excitations or impurity atoms. However, the maximum values of κ_p^s cited by various workers differed noticeably and were several times lower than those calculated under the assumption that the phonons are scattered by the sample surface, while the temperature dependences of $\kappa_p^s(T)$ near T_{\max} varied substantially from sample to sample and could differ strongly from the cubic dependence typical of boundary scattering. A comparison of the temperature dependences of the thermal conductivity κ_p^s of lead crystals above T_{\max} with the predictions of the theory was never made before. The highest values of the electronic thermal conductivity κ_e^n were also different in the different papers.

We have investigated the behavior of the thermal con-

ductivity of lead crystals made of S-000 and S-0000 metal (certified purity⁵ 99.9996% and 99.9999%) from the Chimpent lead plant, in the temperature interval 0.6–7.5 K and in the normal and superconducting states. Some of the measurement results are given in Refs. 1, 6, and 7 (the plot in the abstracts⁷ does not indicate the ordinate scale for the electron mean free paths in lead). The maximum values of the thermal conductivity in the superconducting state of our samples were almost twice as large than those previously cited by others, and the difference of $T = 0.6$ K exceeds one order of magnitude. The measurements have shown that in perfect samples with average diameters $d = 0.4$ and 0.2 cm the thermal conductivity κ_p^s below T_{\max} is indeed proportional to dT^3 and is close to the calculated value, i.e., the effective transport ranges of the phonons at $T < 2$ K are limited by the scattering from the sample surfaces. At the same time the electron ranges in the normal state, calculated from the thermal conductivity κ_e^n , are much lower than the characteristic dimensions $l_e^n \ll d$ and are limited by scattering from the impurity atoms. The ratio of the room-temperature and residual resistances, calculated from the thermal conductivity κ_e^n exceeded 35 000 for the better samples.

A comparison of the experimental data with the predictions of the theory⁸⁻¹² has shown that the results of different calculations of the electronic thermal conductivity κ_{ep}^s of a pure superconductor, which is determined by the scattering of the electronic excitations from the phonons, differ noticeably from one another and do not agree with experiment: the theory predicts a weak change or even a growth of κ_{ep}^s with decreasing temperature near T_c , while the experimental relation is close to $\kappa_{ep}^s \propto T^3$. At the same time the temperature dependence of the phonon component κ_{pe}^s in phonon-electron scattering in a superconductor, calculated from the equations of Geilikman and Kresin,⁹ agreed practically with the curve calculated from the experimental data. The phonon thermal conductivity of lead $\kappa_{pe}^s = 2.5 \cdot 10^{-3} T^2$ W/cm · K, obtained using the approximation $T = T_c$ in the normal state, is close to that previously calculated¹³ from the results of the measurements of the effect of impurities on the thermal conductivity of lead.

We note that despite some differences between the models, the functions $\kappa_{pe}(T)$ predicted by the theories of Bardin *et al.*⁸ and of Geilikman and Kresin⁹ are close to each other. In both papers they neglected the mutual dragging of the quasiparticles, an assumption apparently close to the real situation (the electron mean free paths are small and are limited by the strong scattering from the impurity atoms).

Interest attaches to the results of investigations of the influence of plastic deformation on the thermal conductivity of lead crystals. In all cases the temperature dependence of the electronic thermal conductivity in the normal state below T_{\max} was not altered by deformation, but the phonon thermal conductivity changed appreciably at $T \leq T_{\max}$: the plot of $\kappa_p^s(T)$ of deformed crystals was always steeper than in the initial crystals. Thus, for a sample plastically deformed

in tension by 0.4%, at various temperatures, the $\kappa_p^s(T)$ dependence turned out to be close to $\kappa_p^s \propto T^5$ in the region $2K \geq T \geq 1K$ and at $0.9 \geq T \geq 0.6K$ it was closer to $\kappa_p^s \propto T^3$. This behavior must be attributed to a manifestation of the flutter effect, i.e., scattering of phonons by dislocations that "vibrate" in the stress field of the phonon incident on the dislocation.^{14,15} Moreover, it was shown in Ref. 16 that the natural frequencies of the vibrations of the split dislocations in lead equal 0.15×10^{11} Hz, and in our experiments the change of the slope of the $\kappa_p^s(T)$ curve of the deformed sample occurs at $T \approx 0.9K$ (the frequency of the thermal phonons that dominate at the temperature T is $\nu \approx T \cdot 10^{11}$ Hz).

2. EXPERIMENT

A. Sample preparation

The samples were made of pure lead of brand S-000 and S-0000 from the Chirkent lead plant. According to the plant certificate⁵ the impurity contents are less than 10^{-3} and $10^{-4}\%$, respectively. The sample preparation is described in detail in Ref. 17. The metal initially molten in a quartz funnel in a vacuum of 10^{-6} mm Hg was poured through a thin aperture in a dismountable graphite mold with a cylindrical channel of diameter 2.5 or 6 mm and of length 80 mm, mounted vertically under the vacuum bell. The cylindrical sample was extracted from the mold, placed in a horizontal quartz vessel whose inner surface was roughened and covered beforehand with a thin carbon film, and the freely lying piece was subjected to multiple zone recrystallization in vacuum (the width of the molten zone was ~ 2 cm). The sample prepared in this manner had an oval cross section with axis ratio from 1:1.5 to 1:2. The freshly prepared sample had a mirror-smooth outer surface, which did not become dull after several days in air. The crystals were not oriented, inasmuch as the crystals with fcc structure were sufficiently isotropic. Since the thermal conductivity of the S-000 lead samples was close to that of the better of the previously investigated crystals,⁴ the principal measurements, after debugging the procedures of sample growing and mounting the crystals in the apparatus, were made on samples of S-0000 lead, and the highest thermal conductivity in the normal state was possessed by samples prepared of metal of the same brand from the Collection of Pure Metals of the USSR Academy of Sciences. This points to the possibility and need of further increasing the chemical purity of the lead (we recall that in the better of our samples the electron ranges were $l_{ei}^n \leq 10^{-2}$ cm).

B. Construction of instrument

Two measurement runs were made. At first, during the course of developing the technique of sample preparation and thermometer and heater mounting, the measurements were made in the temperature interval 1.3–7.5 K, while the copper cold finger, to which the sample was soldered, was cooled directly by liquid helium. In the second run, in which the cold finger was part of the copper vessel with the He³, the working interval was increased to 0.6 K. In both cases, the samples were placed in a pan inside the metallic vacuum chamber, on

the outside of which a superconducting solenoid cooled with liquid helium was placed. The solenoid made possible measurements in longitudinal magnetic fields up to 0.5 T (the transverse field component was ≤ 0.05 of the longitudinal one). To eliminate the influence of the frozen-in field on the thermal conductivity, the measurements were first made without a field, and then repeated in a magnetic field (usually $H=0.09$ T).

The vessel, made of a longitudinally cut segment of thin-wall stainless steel tubing of 10 mm diam. \times 0.3 mm, was fastened with silver solder to the end of the cold finger. In the first experiments the samples were soldered to the cold finger, using a soldering iron or a burner and POS-60 solder, after which two thermometers and two heaters were soldered to the sample. Measurements have shown, however, that the sample so mounted could be easily deformed both during the assembly and during the cooling of the setup—owing to the difference between the expansions of the lead and of the stainless steel. The assembly procedure was therefore improved. The surface of the vessel was first covered with a thin teflon film that insulated the sample from the vessel and allowed it to slide freely over the surface when the instrument was cooled. The sample was inserted in the horizontally mounted vessel flush against the end face of the cold finger. The thermometers and heaters were placed in the vessel in such a way that the tinned copper strips connected to them were freely located on the upper surface of the sample. The strips and the end face of the cold finger were tinned beforehand with easy melting solder and covered with a layer of flux, so that when the entire structure was gradually heated to the melting point of Wood's alloy the sample became soldered to the cold duct and the strips were simultaneously soldered to the samples.

The thermometers were 10 Ω , 1/8 W Allen-Bradley carbon resistors tightly wrapped with copper foil glued with epoxy resin. The wire-wound heaters of 100- Ω resistance were made of constantan wire wound and glued on a copper foil strip 10 mm wide. The thermometers were calibrated against the vapor tension of liquid helium and against the superconducting transition point of the lead. Typical values of the temperature difference were 0.003–0.01 K and were measured with accuracy not worse than $\pm 5\%$. To improve the accuracy of the reading at a given point, the measurements were repeated at several different temperature gradients. The effective cross section area of the sample was estimated from the electric resistance of the sample section between the thermometers at room temperature, so that the absolute values of the thermal conductivity were known with accuracy not worse than $\pm 10\%$. Since a low-melting-point alloy was used for soldering, the sample annealing temperature could not exceed 50° in this run. The measurements have shown that for a practically complete annealing of weakly deformed samples it was sufficient to keep the samples at this temperature for one day. To this end, without dismantling the apparatus, we poured into the nitrogen dewar hot water whose temperature was maintained at 50–60 °C.

C. Measurement results

In the first run of experiments the differences between the temperature dependences of the thermal conductivity of our samples were in good agreement with the scatter of the thermal conductivities of pure lead samples as measured by different workers.⁴ Our experiment has shown that in the normal state the maximum thermal conductivity of the samples was practically independent of their dimensions or mounting methods, was changed little by plastic deformation at room temperatures, and was determined mainly by the chemical purity of the initial metal and by the applied magnetic field. In a field $H=0.09$ T the maximum values of the thermal conductivity were 30–50 W/cm·K for S-0000 samples from different batches, and 20–25 W/cm·K for S-000 samples, i.e., the decisive factor in the normal state is the electronic component κ_e^n and the maximum electron ranges are limited by scattering by impurity atoms (charged centers).

In the superconducting state, the thermal conductivity and its temperature dependence at temperatures near and below the maximum of the thermal conductivity could vary significantly from sample to sample at equal purity—they depended on the mounting method and on the sample dimensions, were changed several-fold by deformation and subsequent annealing, but depended little on the chemical purity of the metal, i.e., the maximum thermal conductivity and its temperature dependence for the superconducting samples were determined mainly by the phonon component κ_p^s (the phonons are scattered much more strongly than the electrons by the crystal structure defects, and more weakly

by impurity atoms).

Some of the results obtained in the first run are shown in Fig. 1. Curves 1 and 2 illustrate the change of the thermal conductivity κ_e^n of a cylindrical sample of diameter $d=6$ mm made of S-0000 lead with increase of the longitudinal magnetic field from 0.09 to 0.24 T. Curves 3–7 show the temperature dependence of the thermal conductivity of various samples in the superconducting state. At the very lowest temperatures ($T \leq 1.5$ K, $T/T_c \leq 0.2$) the thermal conductivity of our better samples was several times larger than κ_p^s of the previously investigated crystals⁴ and was close to the calculated phonon thermal conductivity of a crystal having the same diameter. However, the temperature dependence of κ_p^s at temperatures below the maximum of the thermal conductivity of various samples varied in the range $\kappa_p^s \propto T^3 - T^5$ and not in the expected $\kappa_p^s \propto T^n$ with $n \leq 3$, which is typical of phonon scattering from the surface of a single-crystal sample or from individual defects in the interior of the crystal.^{14,18} It is seen from Fig. 1 that not only the dimensions but also the mounting method could influence substantially the behavior of the thermal conductivity κ_p^s of the lead samples, therefore all the subsequent measurements were made on samples mounted in the apparatus in the same manner (gradual heating and cooling, soldering with soft solder, placement on a teflon substrate that allowed the sample to glide freely over the substrate with changing temperature).

The influence of the deformation at room temperatures and of the subsequent annealing on the thermal conductivity of one and the same sample in the superconducting state is illustrated in Fig. 2. Curve 1 shows the thermal conductivity of one of the better samples with dimensions $4 \times 6 \times 75$ mm, curve 2 the thermal conductivity of a sample with dimensions $3.7 \times 6 \times 60$ and having the same purity, but from a different batch, and curve 2' the same sample but plastically deformed by flexure (the free end of the sample was bent 4 mm after the measurement cycle and then again pressed

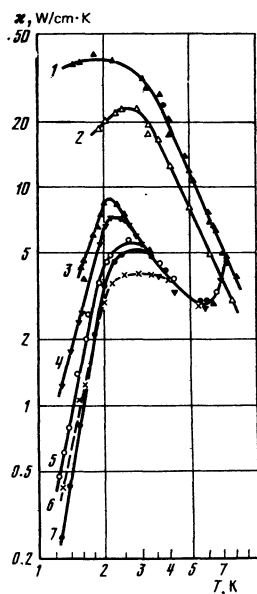


FIG. 1. Influence of applied magnetic field, of the crystal quality, and of the mounting conditions on the thermal conductivity of samples in the normal state (curves 1, 2) and in the superconducting state (curves 3–7). Curves 1, 2—parallel fields $H=0.09$ and 0.24 T; 3, 4—sample of S-0000 lead after one day's annealing at 50°C and prior to annealing (sample diameter 6 mm); 5, 7—samples of 2.5 mm diameter of S-0000 and S-000 lead, respectively; 6—S-000 sample of 6 mm diameter and deformed in the course of mounting.

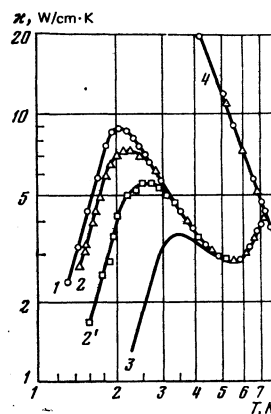


FIG. 2. Comparison of the behavior of the thermal conductivity κ_p^s of samples having close values of the thermal conductivity in the normal state (curve 4): 1—sample of S-0000 metal from the Metal Collection of the USSR Academy of Sciences, 2—sample of commercial S-0000 metal, 2'—the same sample deformed by flexure at room temperature, 3—sample investigated by Montgomery.¹³

against the vessel). After annealing this sample for one day at 50 °C, its thermal conductivity κ_p^s coincided with the initial one (2). Curve 3 shows the thermal conductivity obtained in Ref. 13 a sample having nearly the same dimensions. The plots of the thermal conductivity κ_p^n in the normal state are practically the same for all three samples at $T > 4$ K (curve 4). The deformation produced a small change (less than 10%) in κ_p^n .

In the second run of experiments, the running temperature interval was extended to 0.6 K, and in addition we attempted to determine the influence of the deformation at low temperatures on the thermal conductivity of a perfect crystal. To this end, after performing the cycle of measurements on the perfect sample, its free end was soldered with low-melting solder to the vessel. The sample, 60 mm long and with cross section 3.5 × 7 mm, was fastened at two points at the ends of the crystal. Since the stainless-steel vessel contracts much less when cooled than the lead crystal, the sample cooled from room temperature to that of liquid helium was plastically deformed—it was elongated by ~0.4%, judging from the data of the monograph of Corrucini and Gniewek.¹⁹ This estimate is close to the degree of deformation calculated directly from the sag of the sample (when heated to room temperature the sample became unstable, was bent, and the sag at the center was ~3 mm). After the measurement run the sample was again unsoldered and insulated from the vessel, the sample was straightened out, and annealed for several days at 50 °C. The thermal conductivity of the annealed sample turned out to be close to the initial value.

The results of these measurements are shown in Fig. 3. Curves 1 and 2 show plots of $\kappa_p^n(T)$ of the sample before and after the deformation. The thermal conductivity κ_p^n of the deformed sample after annealing prac-

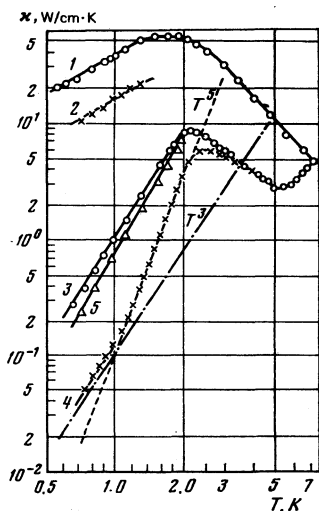


FIG. 3. Influence of deformation at low temperature on the thermal conductivity of pure lead crystals: 1, 2—thermal conductivity in normal state before and after deformation, 3, 4, 5—thermal conductivity of sample in the superconducting state before deformation, of the deformed crystal, and after annealing.

tically coincided with the initial one (curve 1). Curves 3 and 4 are plots of κ_p^s of a perfect and of a deformed sample, while curve 5 is a plot of $\kappa_p^s(T)$ after annealing. The dashed straight line corresponds to the relation $\kappa_p^s \propto T^5$, while the dash-dot line corresponds to the relation $\kappa_p^s \propto T^3$ which is typical of phonons scattering by a crystal surface. It is seen that in the interval 1–2.2 K the thermal conductivity κ_p^s of the deformed sample decreases in proportion to T^5 , while at $T \leq 0.9$ K it is proportional to T^3 . We have indicated above that a stronger-than-cubic dependence was observed in a number of samples of the first run (Fig. 1). Similar relations can be observed also in the comparison of the results obtained by different workers at temperatures above the maximum of the thermal conductivity.⁴ A common result obtained by all is that deformation of lead increases the slopes of the $\kappa_p^s(T)$ curves at temperatures above the maximum of the thermal conductivity.

3. DISCUSSION OF RESULTS

A. Basic theoretical premises⁸⁻¹²

We consider now briefly the predictions of the theory of thermal conductivity of superconductors. In the normal state the thermal conductivity of a superconductor, like that of a normal metal, is determined by the sum of the electronic (κ_e^n) and lattice (κ_p^n) components:

$$\kappa^n = \kappa_e^n + \kappa_p^n, \quad (1)$$

with $\kappa_e^n \gg \kappa_p^n$ in pure metals on account of the phonon-electron scattering. The thermal resistance $(\kappa_e^n)^{-1}$ in the electron system is governed by scattering of the electrons by the phonons $(\kappa_{ep}^n)^{-1}$ and to the summary resistance $\sum_i (\kappa_{ei}^n)^{-1}$ due to the scattering of the electrons by the impurity atoms (charged centers), by defects, and by the sample surface:

$$(\kappa_e^n)^{-1} = (\kappa_{ep}^n)^{-1} + \sum_i (\kappa_{ei}^n)^{-1} = (\alpha/T^2)^{-1} + (\beta T)^{-1}; \quad (2)$$

here α and β are parameters determined by the properties of the material, and by the purity and degree of perfection of the sample. With decreasing temperature, κ_e^n increases in proportion to T^2 (the electron-phonon scattering predominates), reaches a maximum, and then decreases in proportion to T .

Similarly, the thermal resistance in the phonon system is due to phonon-electron scattering, $(\kappa_{pe}^n)^{-1}$, and to phonon scattering by phonons, defects, and impurities in the volume and on the surface of the sample, $\sum_i (\kappa_{pi}^n)^{-1}$; in contrast to the electrons, the temperature dependence of the second term in the expression

$$(\kappa_p^n)^{-1} = (\kappa_{pe}^n)^{-1} + \sum_i (\kappa_{pi}^n)^{-1} = (\gamma T^2)^{-1} + \sum_i (\kappa_{pi}^n)^{-1} \quad (3)$$

depends on which of the phonon-relaxation mechanism prevails in this temperature interval, and is not known beforehand. In perfect crystals at $T > T_{max}$ the principal role is played by phonon-electron scattering and $\kappa_p^n \propto T^2$, while at the lowest temperature the scattering by the sample surface becomes noticeable and $\kappa_p^n \propto dT^3$,

where d is the characteristic dimension of the sample.

In the superconducting state in pure metals near T_c , the electron component κ_{ep}^s exceeds as before the phonon component κ_{pe}^s , but with decreasing temperature the number of electronic excitations n_e decreases rapidly ($n_e \propto e^{-\Delta/T}$, where Δ is the energy gap parameter), so that κ_{ep}^s decreases and the phonon component begins to increase and at sufficiently low temperatures $\kappa_{pe}^s \gg \kappa_{ep}^s$.

Within the framework of the Bardeen-Cooper-Schrieffer theory, Δ depends only on the reduced temperature $t \equiv T/T_c$, so that in the case of identical quasiparticle scattering mechanisms the change of the thermal conductivity following the superconducting transitions can be described in the form of the law of corresponding states: the ratios

$$\kappa_{ei}^s/\kappa_{ei}^n = f(t), \quad \kappa_{ep}^s/\kappa_{ep}^n = g(t), \quad \kappa_{pe}^s/\kappa_{pe}^n = h(t)$$

depend only on the reduced temperature t . Expressions (1)–(3) for the superconducting state can be written in the form

$$\kappa^s = \kappa_e^s + \kappa_p^s, \quad (4)$$

$$\begin{aligned} (\kappa_e^s)^{-1} &= [g(t)\kappa_{ep}^n(t)]^{-1} + \sum_i [f(t)\kappa_{ei}^n(t)]^{-1} \\ &= [g(t)\kappa_{ep}^n(T_c)/t^2]^{-1} + \sum_i [f(t)\kappa_{ei}^n(T_c)t]^{-1}, \end{aligned} \quad (5)$$

$$\begin{aligned} (\kappa_p^s)^{-1} &= [h(t)\kappa_{pe}^n(t)]^{-1} + \sum_i (\kappa_{pi}^n)^{-1} \\ &= [h(t)\kappa_{pe}^n(T_c)t^2]^{-1} + \sum_i (\kappa_{pi}^n)^{-1}, \end{aligned} \quad (6)$$

where $\kappa_{ep}^n(T_c)$, $\kappa_{ei}^n(T_c)$, and $\kappa_{pe}^n(T_c)$ are the values of the corresponding components as $T \rightarrow T_c$. As shown in Refs. 8–11, following the superconducting transition in a zero magnetic field the thermal conductivity varies continuously in first-order approximation (with an error less than 30%), i.e., as $T \rightarrow T_c$

$$\kappa_{ep}^s \rightarrow \kappa_{ep}^n, \quad \kappa_{ei}^s \rightarrow \kappa_{ei}^n, \quad \kappa_{pe}^s \rightarrow \kappa_{pe}^n$$

and by definition the functions $g(t)$, $f(t)$, and $h(t)$ are identically equal to unity at $t \geq 1$.

The explicit expressions for the dependences of f , g , and h on the reduced temperature are unwieldy and obscure. To compare the results with one another and with experiment it is necessary to use computer-calculated plots of these functions.^{8,9,12} The plots of $f(t)$ and $h(t)$ in Refs. 8 and 9, which describe the electronic thermal conductivity κ_{ei}^s of "dirty" superconductors and the phonon thermal conductivity κ_{pe}^s in phonon-electron scattering, agree well with each other. The measured κ_{ei}^s of dirty superconductors in which $\kappa_{ei}^n \ll \kappa_{ep}^n$ at $T \geq T_c$ agree with the theory. A detailed comparison of the behavior of the phonon component κ_{pe}^s was heretofore meaningless in view of the low chemical purity and quality of the samples. The theory was in qualitative agreement with experiment.

The differences between the expressions for the collision integrals and the methods of solving the kinetic equations affected most strongly the results of the cal-

culations of the electronic thermal conductivity κ_{ep}^s of pure superconductors, which is governed by the electron-phonon scattering. The main point is that in all the papers the functions $g(t)$ decrease slowly with decreasing temperature near T_c , so that according to the theory $g(t)/t^2 \geq 1$, whereas in practice in all the experiments κ_{ep}^s decreases rapidly with decreasing temperature [$g(t) \propto t^b$ according to our data]. To reconcile the theory of the superconductivity of pure superconductors with experiment, a number of authors^{10–12} wrote down more accurate collision integrals and took into account the increments due to mutual dragging of the quasiparticles. However, the values of $g(t)$ cited in Ref. 12 differ even more from experiment than before.

Estimates with the aid of the formulas cited by Gurevich and Krylov¹⁰ and by Geilikman and Chechetkin¹¹ show that at temperatures $T \leq 1$ K phonon-electron dragging in lead might increase κ_{ep}^s to a value comparable with the phonon thermal conductivity κ_{pe}^s , but in real samples the phonon mean free paths are limited by scattering from the surface even at $T \approx 2$ K, and those of the electronic excitations are limited by scattering from the impurity atoms (estimates yield $l_{ei}^n \leq 10^{-2}$ cm). It is therefore quite a complicated matter to attempt to separate unambiguously the contribution due to phonon-electron dragging, as is proposed in Refs. 10 and 11, from the results of the measurement of the thermal conductivity of lead samples. We encountered previously a similar situation with bismuth, whose thermal conductivity at helium temperature is likewise determined mainly by phonons that interact weakly with the carriers. In that case the phonon dragging could be easily observed by measuring the dependence of the thermoelectric power on the temperature and on the sample dimensions (a two-step phonon-phonon dragging of the carriers was observed in bulky bismuth crystals). It is clear that to observe phonon-dragging effects in superconductors it is likewise necessary to develop a special observation procedure.

Since the magnitude and the temperature dependence of the gap parameter Δ_{pb} in lead differ little from the value Δ_{BCS} assumed in the BCS model, we have calculated numerically $\Delta_{pb}(T)$ and the functions $f(T)$, $g(T)$, and $h(T)$ for lead, using the equations given in Ref. 9. With accuracy sufficient for our purpose we can state that at $T < T_c$ the parameter $\Delta_{pb} = 1.2\Delta_{BCS}$, with $\Delta_{BCS} = 2.1T_c b$, where b is the root of the equation b

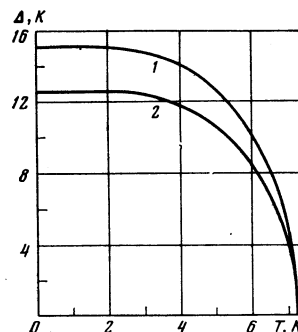


FIG. 4. Calculated dependence of the gap parameter Δ_{pb} in lead on the temperature (1) and the plot in the BCS model (2).

$=\tanh(tb)$, and as $T \rightarrow T_c$ it is more accurate to use the relation $\Delta_{pb} \approx 2.15T(1-t)^{1/2} \approx 1.4\Delta_{BCS}$. The calculated Δ_{pb} are shown in Fig. 4 (curve 1), which shows also the plot for the BCS model (curve 2).

Figure 5 shows the calculated functions $f(T)$, $g(T)$, and $h(T)$ (curves 1, 2, and 3) and the experimental plot of $g(T)$ (curve 4; the dashed curve shows $g(T)$ under the assumption that the phonon thermal conductivity behaves in agreement with the calculations). The points along the $h(T)$ curve were calculated from the experimental results (see the next section). It is seen that the points fit in practice the theoretical curve. The dash-dot curve shows the variation of $h(T)$ near T_c in the more accurate model for Δ_{pb} . The points on the $f(T)$ curve correspond to the thermal conductivity of dirty lead ($\sim 0.02\%$ Bi) and were calculated by us from the data of Ref. 20, i.e., as indicated above, the functions $h(T)$ and $f(T)$ calculated from the formulas of the monograph of Gilikman and Kresin⁹ agree well with experiment.

B. Comparison of theory with experiment. Normal state

As seen from Figs. 1–3, the temperature dependences of κ_e^n in the interval 0.6–7.5 K agree qualitatively with that predicted by Eq. (2), viz., electron-phonon scattering predominates above 2 K, and scattering by impurity atoms predominates at $T < 2$ K. For example, the thermal conductivity of one of the better crystals (Fig. 3) in a field $H=0.09$ T can be described by the expression

$$(\kappa_e^n)^{-1} = (420 T^{-2.3})^{-1} + (40 T)^{-1} \quad [\text{W/cm}\cdot\text{K}]^{-1}. \quad (7)$$

Since the matrix element for the description of electron-phonon interaction in concrete metals are un-

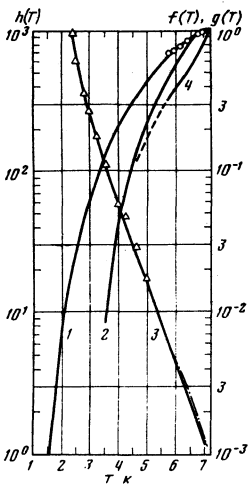


FIG. 5. Calculated ratios of the thermal conductivity of lead in the superconducting and normal states: 1—scattering by impurities [$f(T)$], 2—electron scattering by phonons [$g(T)$], 3—phonon scattering by electronic excitations [$h(T)$]; curve 4 corresponds to the function $g(T)$ calculated from the experimental data (Fig. 3). Points on curve 3—ratio $\kappa_{pe}^s/\kappa_{pe}^n$ calculated from the experimental data (Figs. 3 and 2); the points on curve 1 correspond to the thermal conductivity of lead with 0.02% of bismuth impurity.

known, no exact quantitative calculations of κ_{ep}^n in lead were made. A formula in the form

$$\kappa_{ep}^n = 0.015 n_e^{-2/3} (\Theta/T)^2 \kappa_{ep}^n(\infty),$$

(n_e is the number of free electrons per atom and $\kappa_{ep}^n(\infty) = 0.35 \text{ W/cm}\cdot\text{K}$ is the thermal conductivity at $T \gg \Theta$), which was used in the theory¹⁴ to describe the electronic thermal conductivity of metal, is suitable only for qualitative estimates and underestimates the thermal conductivity of lead at $T = T_c$ by a factor 13.

The slopes of the $\kappa_{ep}^n(T)$ curves for different samples can differ somewhat both in our experiment and in accord with the data by others.⁴ On the average, in fields $H=0.09$ – 0.1 T, the data obtained by various authors are close to the relation

$$\kappa_{ep}^n \propto T^{-2.8 \pm 0.4},$$

i.e., they are much steeper than the quadratic plots predicted by the theory. Allowance for the influence of the magnetic field on the thermal conductivity can only increase the exponent even more.

To estimate the magnetoresistance, we measured the thermal conductivity of the same sample in fields 0.09 and 0.24 T (Fig. 1). In accord with the Kohler rule, the change of the thermal conductivity upon application of a magnetic field is given by

$$\frac{\kappa_e^n(0) - \kappa_e^n(H)}{\kappa_e^n(H)} = \text{const} \cdot \frac{H^n}{T}, \quad (8)$$

where $\kappa_e^n(0)$ and $\kappa_e^n(H)$ are the thermal conductivities in a zero field and in a field H , while the exponents and the proportionality coefficients can vary somewhat when with change of the principal relaxation mechanism, of the field, and of the sample orientation (saturation is possible). Putting $n=2$, we have found that the values of the proportionality coefficient vary smoothly over the entire temperature range and amount to $40 \pm 15 \text{ T}^2/\text{K}$ with a minimum in the center of the interval near the maximum of the thermal conductivity. The values of the coefficient at $n=1$ vary similarly, but the obtained values of $\kappa_e^n(0)$ are then somewhat higher than for a quadratic dependence. In all variants, the correction for the magnetoresistance is $\leq 10\%$ near T_c and becomes comparable with the measured quantity $\kappa_e^n(H)$ at $T \leq 1$ K. Therefore only qualitative estimates of $\kappa_e^n(0)$ are meaningful at $T \leq 1$ K, namely, at $T = 0.6$ K we have $\kappa_e^n(0) \leq 3\kappa_e^n(0.09)$.

The deviation of $\kappa_{ep}^n(T)$ from a quadratic dependence can be due either to the 15% increase of the Debye temperature in the interval 10–2 K, or to phonon-electron dragging effects. As will be shown subsequently, the conditions $\tau_{pe} \gg \tau_{ep}$ necessary for this to occur in lead are satisfied in the indicated temperature interval (τ_{pe}, τ_{ep} are the relaxation times for mutual scattering of the quasiparticles), but an unambiguous assessment of the role of dragging effects from the temperature dependence alone is quite difficult.

The effective transport mean free paths of the electrons and phonons, l_e and l_p , and the corresponding

relaxation times τ_e and τ_p , can be estimated by using the known relations

$$\kappa_e^n = 1/3 C_s v_F l_e^n = 1/3 C_s v_F^2 \tau_e, \quad (9)$$

$$\kappa_p^n = 1/3 C_p s l_p^n = 1/3 C_p s^2 \tau_p, \quad (10)$$

where C_s and C_p are the specific heats of the electron gas and of the lead lattice, respectively, v_F is the electron Fermi velocity and s is the average speed of sound in the Debye approximation. Substituting the values¹⁸

$$C_s = 1.6 \cdot 10^{-4} T \text{ J/cm}^3 \cdot \text{K}, \quad C_p = 1.06 \cdot 10^{-4} T^3 \text{ J/cm}^3 \cdot \text{K}, \\ v_F = 1.8 \cdot 10^8 \text{ cm/sec}, \quad s = 1.05 \cdot 10^5 \text{ cm/sec},$$

we get

$$\kappa_e^n = 10^4 T l_e^n = 1.8 \cdot 10^{13} T \tau_e^n \text{ W/cm} \cdot \text{K}, \quad (11)$$

$$\kappa_p^n = 3.7 T^3 l_p^n = 3.9 \cdot 10^3 T^3 \tau_p^n \text{ W/cm} \cdot \text{K}. \quad (12)$$

(Similar estimates of the quasiparticle mean free paths are given in Ref. 21.) From this, in accord with (2) and (7), we have for the best of the samples in a field $H = 0.09 \text{ T}$

$$l_e^n = 4.2 \cdot 10^{-2} T^{-3.3} \text{ cm}, \quad \tau_e^n = 2.3 \cdot 10^{-10} T^{-3.3} \text{ sec} \\ l_p^n = 4 \cdot 10^{-3} \text{ cm}, \quad \tau_p^n = 2.2 \cdot 10^{-11} \text{ sec}. \quad (13)$$

It follows from the estimates (8) that for any approximation to a zero field we have $l_e^n \leq 1.2 \cdot 10^{-2} \text{ cm} \ll d$, i.e., the electrons are scattered by the impurity atoms and not by the sample surface, even in the purest of the investigated S-0000 crystals.

In the S-000 and S-0000 samples, the thermal conductivity due to electron scattering by impurities amounted to $\kappa_{ei}^n \approx (20-40)T \text{ W/cm} \cdot \text{K}$ [Figs. 1-3, formula (7)]. These values agree well with estimates of the influence of the impurities on the thermal conductivity of lead. Thus, the thermal conductivity of a lead sample with 0.02% bismuth was found to be²⁰ $\kappa_{ei}^n = 0.3T \text{ W/cm} \cdot \text{K}$ in the same fields as in our case, i.e., it was lower by a factor 100 than in our samples. According to Ref. 13, the average thermal conductivity of lead containing $x_i\%$ impurity atoms is $\kappa_{ei}^n = x_i^{-1} \cdot (0.3-3)T \cdot 10^{-2} \text{ W/cm} \cdot \text{K}$. This estimate is close to the values of κ_{ei}^n in normal metals, which can be obtained by using the Wiedemann-Franz law

$$\kappa_{ei}^n = LT/\rho_i \approx (0.24-2.4) T x_i^{-1} \cdot 10^{-2} \text{ W/cm} \cdot \text{K}, \quad (14)$$

where $\rho_i = (1-10) \cdot 10^{-6} x_i \Omega \cdot \text{cm}$ is the residual resistance of a metal containing $x_i\%$ impurity atoms,¹⁴ and $L = 2.4 \cdot 10^{-8} \text{ W} \cdot \Omega/\text{K}^2$ is the Lorentz number. It is seen that the two estimates of κ_{ei}^n (from Eq. (14) and from the direct measurements^{13, 20}) agree in order of magnitude with each other and with the estimates of κ_{ei}^n calculated for our samples from the certified values. The ratio, calculated from (14), of the room-temperature resistivity (ρ_{300}) to the residual resistivity is $\rho_{300}/\rho_i = 3.5 \cdot 10^4$ for the better samples (when a zero field is approached, $\rho_{300}/\rho_i \leq 10^5$).

The phonon thermal conductivity of lead at $T \geq T_c$, calculated¹³ from the measurements of the effect of impurities on the thermal conductivity of the samples, was $\kappa_{pe}^n = 1.3 \cdot 10^{-3} T^2 \text{ W/cm} \cdot \text{K}$. According to our estimates given in the next section, $\kappa_{pe}^n = 2.5 \cdot 10^{-3} T^2 \text{ W/cm} \cdot \text{K}$ (the difference between the numbers may be due to differences in the chemical purity of the metals). Us-

ing relation (12), we get $l_p^n = 6.7 \cdot 10^{-4} T^{-1} \text{ cm}$ and $\tau_p^n = 6.4 \cdot 10^{-9} T^{-1} \text{ sec}$, i.e., $\tau_p^n \gg \tau_{ep}^n$ in the interval 2-8 K, and according to Refs. 10 and 14 an important role in the mutual scattering of the quasiparticles in lead can be played by phonon-electron dragging effects. We note that just as in the case of the electronic thermal conductivity, no theoretical calculations of κ_{pe}^n in lead were made, and the cited^{14, 11} estimating formulas of the type

$$\kappa_{pe}^n = (3.7/n_e^2) (T/\theta)^2 \kappa_{ep}^n(\infty) = 7 \cdot 10^{-5} T^2 \text{ W/cm} \cdot \text{K}$$

yield a value of κ_{pe}^n smaller than the experimental one by a factor of 30.

C. Comparison of theory and experiment. Superconducting state

The maximal thermal conductivity of lead samples in the superconducting state, as follows from our plots (Figs. 1-3) and the published data,⁴ depends little on the chemical purity of the metal, at an impurity concentration $x_i < 10^{-2}\%$ in contrast to the thermal conductivity in the normal state, but can vary greatly from sample to sample when changes occur in the mounting conditions, in the degree of perfection, and in dimensions of samples of like purity, i.e., the principal role below 5 K is played, as follows from various experiments, by the phonon component of the thermal conductivity κ_p^s (the transport free paths of the electrons in elastic scattering by impurity atoms and defects are not changed on going to the superconducting state^{8, 9}; the electrons are scattered much more strongly than the phonons from charged centers). In a perfect crystal the largest phonon free paths are limited by scattering from the sample surface, $l_{pi}^s \leq d$ (the size effect in the thermal conductivity). Substituting in (12) the values $d = 0.4$ and 0.2 cm , we get $\kappa_{pi}^s = (1.4 \text{ and } 0.7) \cdot T^3 \text{ W/cm} \cdot \text{K}$ in agreement with the measurement results on our samples (Fig. 1) at $T \leq 1.5 \text{ K}$. The thermal conductivity of our samples at temperatures below the maximum point T_{\max} of the thermal conductivity is several times higher than the thermal conductivity of the previously investigated samples, and the position of T_{\max} is shifted towards substantially lower temperatures, i.e., the previously investigated⁴ crystals were of much lower quality.

The decrease of the phonon thermal conductivity with increasing temperature at $T > T_{\max}$ can be due to scattering of the phonons in the volume by electronic excitations or by point defects (isotopic scattering, scattering by impurity atoms). Estimates of κ_{pi}^s in isotopic scattering show that $\kappa_{pi}^s \geq 40T^{-1} \text{ W/cm} \cdot \text{K}$, i.e., at $T > 2 \text{ K}$ the isotopic scattering in our samples can still be neglected, and the principal role in chemically pure samples should be assumed by phonon-electron scattering in the volume. Writing in accord with Eq. (6) for samples of 0.4 cm diameter

$$(\kappa_p^s)^{-1} = (\kappa_{pe}^s)^{-1} + (1.4 T^3)^{-1} [\text{W/cm} \cdot \text{K}]^{-1},$$

we can calculate κ_{pe}^s from the experimental data and compare the obtained values with the theoretical ones. As seen from Figs. 2 and 3, at $T > 4 \text{ K}$ we must take into account the contribution of the electronic component

κ_{ep}^s to the experimentally measured total thermal conductivity [Eq. (4)]. The values of κ_{ep}^s were obtained by approximating the $\kappa_{ep}^s(T)$ curve that describes the course of the thermal conductivity in the interval 6–7.2 K in the region of lower temperatures.

The theory^{8,9} describes only the behavior of the ratio $\kappa_{pe}^s/\kappa_{pe}^n = h(T)$ at $T < T_c$. To find the value of κ_{pe}^n we have assumed that the theoretical and experimental values of κ_{pe}^s coincide at 3 K, where the influence of all the corrections is minimal, as seen from Figs. 2 and 3. The resultant value $\kappa_{pe}^n = 2.5 \cdot 10^{-3} T^2$ W/cm·K is half that cited in Ref. 13, a fact readily explained by the influence of phonon-impurity scattering on the results of the estimates in Ref. 13.

The values of $h(T)$ calculated from the experimental data are given in Fig. 5 (the points along curve 3). It is seen that the theoretical and experimental $h(T)$ agree in the wide temperature interval from 2 to 5 K. The agreement between the calculated and experimental $\kappa_{pe}^s(T)$ at $T \leq 5$ K confirms in turn the possibility of approximating the experimental κ_{ep}^s curve from the region $T > 6$ K into the region of lower temperatures.

Near T_c , in a pure sample, the principal role is played by the electronic component κ_{ep}^s , while in a dirty one it is played by κ_{ei}^s (according to Refs. 13 and 20, impurity scattering at $T \sim T_c$ plays the principal role if $x_i \geq 10^{-2}\%$). Since the calculated $\kappa_{ep}^s(T)$ of various authors⁸⁻¹² differ greatly from one another and do not agree with the results of the earlier experiments,⁴ it was of interest to compare the experimental curves of $g(T) = \kappa_{ep}^s/\kappa_{ep}^n$ obtained from our data and of $f(T) = \kappa_{ei}^s/\kappa_{ei}^n$ from the data of Mendelssohn and Olsen²⁰ with the theoretical ones.

As seen from Fig. 5, in a pure sample $g(T) \propto T^5$, i.e., it decreases with decreasing temperature much more rapidly than predicted by the theory. At the same time the values of $f(T)$ calculated from the thermal conductivity of a sample containing 0.02% bismuth agreed well with the theory (the points on the $f(T)$ curve in Fig. 5). Thus, in the superconducting transition the cross section for scattering of electrons by impurity atoms remains constant in first-order approximation, in accord with the theory, while in scattering by phonons near T_c the effective scattering cross section increases much more strongly than predicted by the theory. It appears that in the calculation of κ_{ep}^s of lead one must take into account the fact that the state density of the transverse phonons has a maximum near T_c , as is proposed in Ref. 22. The dashed curve of Fig. 5 shows the experimental $g(T)$ curve approximated in the region $T < 6$ K. The experimental curve approaches the theoretical one with decreasing temperature.

D. Effect of plastic deformation on the thermal conductivity of lead crystals

In contrast to bismuth crystals,²³ flexure deformation at room temperature had practically no effect on the electric conductivity of even the purest lead crystals (the electric conductivity of bismuth at helium temperature and at the same flexure decreased by one-half), but could lead to a decrease of the maximum phonon

thermal conductivity and, most importantly, to a change of the temperature dependence below T_{max} . The important factor here is that unlike in the usually observed phonon thermal conductivity (e.g., that of bismuth crystals), the slopes of the $\kappa_{pi}^s(T)$ curves in deformed samples are steeper than in the initial ones. A similar behavior of κ_{pi}^s was observed also before⁴ and was attributed either to a manifestation of the contribution of the electronic component κ_{ep}^s (second gap,⁹ phonon-electron dragging¹⁰) or to scattering of phonons by dislocation nets.¹³ It is clear from the foregoing, however, that κ_{ep}^s is small at $T \leq 2$ K, and the dragging effects are also negligibly small because of the strong electron-impurity scattering in this region. The second assumption is also unlikely, since the density of the dislocations introduced at a sag of 3–4 mm is small, $N_d \leq 10^7$ cm⁻², and the characteristic wavelengths of the thermal phonons at $T = 1$ K (on the order of a hundred interatomic distances) is much less than the distance between the individual dislocations. Annealing increased the thermal conductivity κ_{pi}^s practically to its initial value, and if the annealing time was not enough then the slope of the curve was also steeper than in the initial state, i.e., the principal role was played by scattering from individual impurities.

The thermal conductivity of a perfect sample and of one deformed by tension at low temperatures, and the effective electron and phonon transport free paths (l_e and l_p) calculated from Eqs. (11) and (12) are shown in Figs. 3 and 6. Assuming that the electronic thermal conductivity of a deformed sample is determined at $T \leq 1.5$ K by scattering from dislocations, $\kappa_{ed}^n = 16T$ W/cm·K, and using the Wiedemann-Franz law $\kappa_{ed}^n = LT/\rho_d$, where $\rho_d = (1 - 10) \times 10^{-19} N_d \Omega$ -cm is the resistivity of the normal metal as determined by electron scattering by the dislocations,¹⁴ we obtain for the density of the introduced dislocations $N_d \approx (0.1 - 1) \times 10^{10}$ cm⁻², i.e., a value higher by two or three orders of magnitude than that obtained from the relative elongation of the sample. The cause of such an appreciable dis-

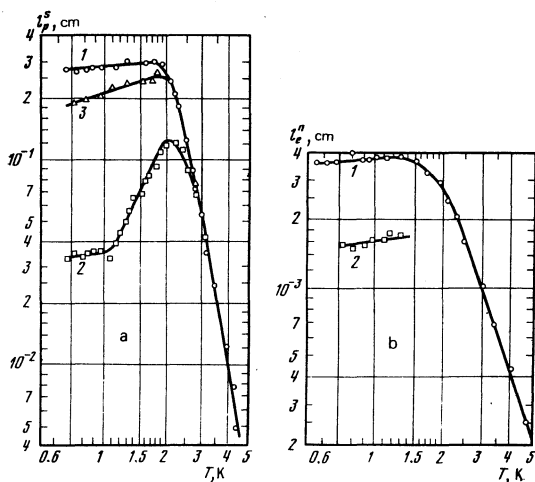


FIG. 6. Effective transport free paths of phonons (a) and electrons (b) in a perfect and in a deformed sample, calculated from the curve of Fig. 3: a) curve 1—initial sample, 2—deformed, 3—annealed; b) curve 1—initial sample, 2—deformed sample.

crepancy in the estimates of N_d may be that the Wiedemann-Franz law does not hold in the presence, say, of small-angle scattering of electrons by dislocations, a process accompanied by a change in the electron energy by an amount on the order of kT , which does not affect the electric conductivity but can play an important role in the establishment of the thermal equilibrium. Unfortunately, no theoretical investigations of the influence of such an inelastic scattering on the thermal conductivity are known to us.

As seen from Fig. 6a, the effective phonon mean free path at temperature below the maximum of the thermal conductivity in a perfect sample is limited by scattering from the surface and is practically independent of temperature, in a deformed sample $l_{pd}^s \propto T^2$ at $1 \text{ K} \leq T \leq 2 \text{ K}$ and $l_{pd}^s \approx \text{const}$ at $0.6 \text{ K} \leq T \leq 0.9 \text{ K}$, and nearly approaches the initial value after annealing. We attribute the observed behavior of l_{pd}^s to the appearance of the flutter effect, i.e., to scattering of the phonons by dislocations by the dislocations that vibrate in the field of the incident phonon,¹⁴ inasmuch as any mechanism of phonon scattering by immobile single microscopic defects would lead to an increase of the mean free path with increasing temperature (the phonon wavelength increases with decreasing temperature). Incoherent small-amplitude thermal oscillations (phonons), in contrast to acoustic waves, are hardly capable of displacing the dislocation as a whole, and the dislocation vibrates within the Peierls relief. If the Peierls force $F_p \ll M\nu^2(a/2\pi)$ that restrains the dislocation (where $M \approx \rho b^2$ is the dislocation mass, ρ is the specific density of the crystal, b is the Burgers vector, and ν is the frequency of the phonon incident on the dislocation), then the radius of phonon scattering by the vibrating dislocation, $\mathcal{F}_{pd}^{ph} \sim S/\nu \sim aT^{-1}\vartheta$ cm, is much larger than the radius of phonon scattering by the stress field around an immobile dislocation, $\mathcal{F}_{pd}^{st} \sim 40bT\vartheta^{-1}$ cm.¹⁴ At lower frequencies the phonon energy is insufficient to excite the oscillations, and the scattering radius \mathcal{F}_{pd}^{ph} turns out to be the same as in scattering by the core of an immobile dislocation, and much less than \mathcal{F}_{pd}^{st} .

Thus, whether the flutter effect appears in the phonon thermal conductivity or the principal role is played by scattering from the stress fields around immobile dislocations depends on the value of F_p and on the characteristic temperatures at which the phonon-dislocation scattering becomes predominant.

Since the principal role is played by scattering of thermal phonons whose frequency is $\nu \approx 10^{11} T$ Hz, to observe the flutter effect at $T \sim 1 \text{ K}$ we must have $F_p \ll 3 \text{ dyn/cm}$. Hence the maximum shear stress $\sigma_c = F_p/b$ needed for the dislocation to start to move in the glide plane, must be $\sigma_c \ll 6 \cdot 10^7 \text{ dyn/cm}^2$ or $\sigma_c \ll 10^{-3}G$, which is certainly true in lead (G is the shear modulus of lead and $\approx 5 \cdot 10^{10} \text{ dyn/cm}^2$). In deformed bismuth crystals the effective phonon mean free path increases with decreasing temperature: $l_{pd}^s \propto T^{-1}$, i.e., the principal role is played by scattering from stress fields around immobile dislocations. In fact, the dislocation density in bismuth, obtained from the known

radius \mathcal{F}_{pd}^{st} , agreed well with the values of N_d estimated from the electric conductivity.²² It can therefore be concluded that in bismuth $F_p \geq 3 \text{ dyn/cm}$ and $\sigma_c \geq 6 \cdot 10^7 \text{ dyn/cm}^2$, in full agree with the difference between the mechanical properties of lead crystals (highly plastic at helium temperatures) and bismuth crystals (brittle already at nitrogen temperatures).

The dislocations vibrating in the field of the elastic wave can absorb and emit phonons, so that we can speak of the presence of local vibrational modes connected with the dislocations. For example, as shown in Ref. 16, in split dislocations one can excite internal periodic vibrations with natural frequencies proportional to the energy of the stacking faults and amounting to $\sim 10^{10}$ Hz for ordinary fcc metals. In lead, according to estimates,¹⁶ the frequency of these dislocation vibrations is 0.15×10^{11} Hz, i.e., in addition to the effect considered above one should observe at temperatures $T \sim 1 \text{ K}$ also resonant absorption of part of the phonons by the vibrating dislocation, and this should lead to a stronger-than-linear dependence of $\kappa_{pd}^s(T)$ in the temperature region near resonance, in accord with our measurements. In the study of the flutter effect, the advantage of lead over normal fcc metals is that at $T \ll T_c$ in the superconducting state the phonon component of the thermal conductivity is decisive and, furthermore, the electron deceleration of the dislocations becomes negligibly small.¹⁶

4. CONCLUSION

Thus, from the thermal conductivity of lead samples in the superconducting and normal states we can assess the effective transport free paths of the phonons and electrons and the relaxation times of the quasiparticles as they are scattered by one another and by defects and impurities within the same sample. In the normal state $\tau_{pe}^n = 6 \cdot 10^{-9} T^{-1}$ sec and $\tau_{pe}^n = 2.3 \cdot 10^{-10} T^{-3.3}$ sec. In the superconducting state the number of electronic excitations decreases exponentially with decreasing temperature, so that τ_{pe} can only increase, and the electron relaxation time decreases because of the increased effective cross section for the scattering of the electronic excitations by the phonons. Thus, in the entire working-temperature interval we have $\tau_{pe} \gg \tau_{ep}$ and, in agreement with the theory,^{10,11} in sufficiently bulky pure lead samples one should expect manifestations of electron-phonon dragging, i.e., it is of interest to investigate further and to increase significantly the chemical purity of the samples. In the investigated S-0000 lead samples, the electron transport free paths were not large enough, $l_{ei}^n \leq 10^{-2}$ cm, for a substantial manifestation of dragging effects in the thermal conductivity.

Figure 7 shows the experimental plot of the thermal conductivity of a perfect sample of 0.4 cm diameter in the superconducting state (curve 1), and also the calculated dependences of the phonon thermal conductivity in size scattering (3) and phonon scattering by electronic excitations (4). It is seen that the calculated and experimental dependences of $\kappa_p^s(T)$ are in good agreement. At the same time the theoretical and experimental electronic components $\kappa_{ep}^s(T)$ differ substantially near T_c .

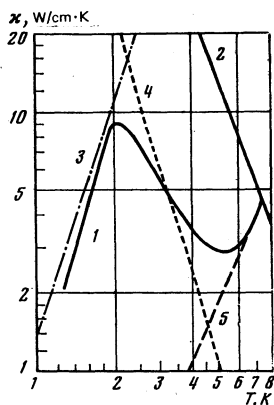


FIG. 7. Contribution of various mechanisms to the thermal conductivity of a perfect lead sample with average diameter 4 mm in the superconducting state (curves 3–5). 1—Experimental plot of $\kappa^s(T)$; 2—experimental plot of $\kappa_{ep}^n(T)$; 3—contribution of size scattering of phonons, 4—thermal conductivity κ_{pe}^s of pure metal, 5—electronic component κ_{ep}^s of the thermal conductivity from the experimental data.

In perfect samples in the superconducting state the effective mean free path of the phonons is limited by the size scattering. In deformed samples, judging from the singularities in the temperature dependence of the thermal conductivity, the decisive phonon-scattering mechanism at $T \approx 1$ K is the flutter effect, i.e., scattering by vibrating dislocations (induced vibrations of the oscillations in an alternating stress field). The singularities induced in the phonon thermal conductivity by phonon scattering by vibrating dislocations were observed also previously in plastically deformed samples of Nb,²⁴ Pb,²⁵ and copper alloys.²⁶

The author thanks A. V. Lokhov, V. N. Khlopinskiĭ, G. V. Iosilevskaya, A. P. Fledotov, and Yu. L. Rodin for help with the experiments and with the computer calculations.

¹L. P. Mezhov-Deglin, in: *Metally vysokoi chistoty (High-Purity Metals)*, Ch. V. Kopetskiĭ, ed., Nauka, 197, pp. 60–

73.

- ²L. P. Mezhov-Deglin, *Zh. Eksp. Teor. Fiz.* **49**, 66 (1974) [*Sov. Phys. JETP* **22**, 47 (1974)].
- ³L. P. Mezhov-Deglin, V. N. Kopylov, and E. S. Medvedev, *Zh. Eksp. Teor. Fiz.* **67**, 1123 (1974) [*Sov. Phys. JETP* **40**, 557 (1975)].
- ⁴G. E. Childs, L. J. Ericks, and R. L. Powell, *Thermal Conductivity of Solids at Room Temperature and Below*, NBS Monograph 131, 1973.
- ⁵L. F. Kozin, in Ref. 1, pp. 162–211.
- ⁶L. P. Mezhov-Deglin, *Pis'ma Zh. Eksp. Teor. Fiz.* **27**, 520 (1978) [*JETP Lett.* **27**, 489 (1978)].
- ⁷L. P. Mezhov-Deglin, *J. de Phys.* **39**, C6-1019 (1978).
- ⁸J. Bardeen, G. Rickayzen, and L. Tewordt, *Phys. Rev.* **113**, 982 (1959).
- ⁹B. T. Geilikman and V. Z. Kresin, *Kineticheskie i nestatsionarnye yavleniya v sverkhprovodnikakh (Kinetic and Nonstationary Phenomena in Superconductors)*, Nauka, 1972 [Halsted, 1974].
- ¹⁰L. E. Gurevich and E. T. Krylov, *Zh. Eksp. Teor. Fiz.* **68**, 1337 (1975) [*Sov. Phys. JETP* **41**, 665 (1975)].
- ¹¹B. T. Geilikman and V. R. Chechetkin, *Zh. Eksp. Teor. Fiz.* **70**, 1884 (1976) [*Sov. Phys. JETP* **43**, 981 (1976)].
- ¹²B. T. Geilikman, V. R. Chechetkin, and M. I. Dushenat, *ibid.* **73**, 2319 (1977) [**46**, 1213 (1977)].
- ¹³H. Montgomery, *Proc. Roy. Soc. A* **244**, 85 (1958).
- ¹⁴J. M. Ziman, *Electrons and Phonons*, Oxford, 1960.
- ¹⁵V. I. Al'shitz and V. L. Indenbom, *Usp. Fiz. Nauk* **115**, 3 (1972) [*Sov. Phys. Usp.* **18**, 1 (1972)].
- ¹⁶H. Kronmüller, *Phys. Stat. Sol. (b)* **52**, 231 (1972).
- ¹⁷L. P. Mezhov-Deglin and V. E. Kopylov, *Prib. Tekh. Éksp.* No. 1, 230 (1975).
- ¹⁸C. Kittel, *Introduction to Solid State Physics*, Wiley, 1976.
- ¹⁹R. J. Corrucini and J. J. Gniewek, *Thermal Expansion of Technical Solids at Low Temperatures*, NBS Monograph 29, 1961.
- ²⁰K. Mendelssohn and J. L. Olsen, *Phys. Rev.* **80**, 859 (1950).
- ²¹V. P. Peshkov and A. Ya. Parshin, *Zh. Eksp. Teor. Fiz.* **48**, 393 (1965) [*Sov. Phys. JETP* **21**, 258 (1965)].
- ²²V. Ambegaokar and J. Woo, *Phys. Rev.* **139**, A1818 (1965).
- ²³V. N. Kopylov and L. P. Mezhov-Deglin, *Fiz. Tverd. Tela (Leningrad)* **15**, 13 (1973) [*Sov. Phys. Solid State* **15**, 8 (1973)].
- ²⁴A. C. Anderson and S. Smith, *J. Phys. Chem. Sol.* **34**, 11 (1973).
- ²⁵B. B. O'Hara and A. C. Anderson, *Phys. Rev. B* **110**, 574 (1974).
- ²⁶M. Kusunoki and H. Suzuki, *J. Phys. Soc. Jpn* **26**, 932 (1969).

Translated by J. G. Adashko